

# Spontaneous Parametric Down Conversion of Photons Through $\beta$ -Barium Borate

A Senior Project

By

Luke Horowitz

Advisor, Dr. Glen D. Gillen

Department of Physics, California Polytechnic University SLO

May 24, 2016

Approval Page

**Title: Parametric Down Conversion of Photons Through  $\beta$  - Barium Borate**

**Author: Luke Horowitz**

**Date Submitted: May 24, 2016**

Senior Project Advisor: Dr. Glen D. Gillen

---

Signature

---

Date

# Contents

<b>1</b>	<b>Introduction</b>	<b>6</b>
<b>2</b>	<b>Theory</b>	<b>6</b>
2.0.1	Linear and Nonlinear Optics Primer . . . . .	6
2.0.2	Non-Linear Optics and SPDC . . . . .	8
2.0.3	Phase Matching . . . . .	10
<b>3</b>	<b>Experiment</b>	<b>12</b>
3.1	List of Equipment . . . . .	12
3.2	Experimental Setup . . . . .	13
3.2.1	Optics . . . . .	13
3.2.2	BBO Crystal . . . . .	14
3.2.3	Electronics . . . . .	16
3.3	Procedures . . . . .	17
<b>4</b>	<b>Conclusions</b>	<b>17</b>
<b>5</b>	<b>Future Work</b>	<b>18</b>

## List of Tables

1	Acronyms . . . . .	5
2	Type I vs Type II Phase Matching . . . . .	11
3	Equipment . . . . .	12

## List of Figures

1	a) General DFG, b) SPDC with crystal geometry, c) Energy level diagram for SPDC, d) Momentum conservation for SPDC . . . . .	8
---	------------------------------------------------------------------------------------------------------------------------------	---

2	Phase matching angle $\theta$ for SPDC where the ordinary polarization is normal to the page, and the extraordinary polarization is in the plane of the page as illustrated. . . . .	11
3	Optical Path Block Diagram . . . . .	13
4	Mount for BBO crystal . . . . .	15
5	Block diagram of electronics showing the how coincidence counts are obtained from the APD's. . . . .	16

Acronym	Meaning
BBO	$\beta$ -Barium Borate Crystal ( $\beta$ -BaB <sub>2</sub> O <sub>4</sub> )
SFG	Sum Frequency Generation
DFG	Difference Frequency Generation
OR	Optical Rectification
c.c.	Complex Conjugates
SHG	Second Harmonic Generation
SPDC	Spontaneous Parametric Down Conversion
MI	Michelson Interferometer
APD	Avalanche Photodiode
SCA	Single Channel Analyzer
HeNe	Helium-Neon Laser

Table 1: Acronyms

# 1 Introduction

In most undergraduate physics programs, there are usually few opportunities for students to do meaningful laboratory work, especially not in unconventional subjects like quantum mechanics or applied optics. For students who are interested in these subjects, a “hands-on” experiment can be an invaluable learning tool to help them understand difficult concepts. Galvez, *et al.*, [1] present an apparatus for detecting photons that undergo quantum entanglement that can be constructed within a reasonable budget of an undergraduate physics lab. This apparatus can be used to perform a number of different experiments and would be an excellent addition to an advanced physics laboratory curriculum. Building this apparatus is relevant because it can be used to teach both advanced theoretical physics like non-linear quantum optics as well as advanced experimental techniques in optics and electronics. I was motivated to do this project because of what I learned in Dr. Glen D. Gillen’s Advanced Optics course at Cal Poly SLO. I wanted to get more experience with experimental optics and was interested in exploring the non-linear relationships that connect optics and quantum mechanics.

## 2 Theory

### 2.0.1 Linear and Nonlinear Optics Primer

Laser light is an oscillating and traveling electromagnetic wave with specific spatial and temporal parameters  $k$  and  $\omega$ , respectively. The temporal parameter is the angular frequency,  $\omega$ , and the spatial parameter is the wavenumber,  $k$ , and they are related via the equation  $\omega = vk$ , where  $v$  is the speed of light in the medium. The relevant information about the wave is contained in the electric part of the electromagnetic wave, which, in this case, is mathematically convenient to express as a complex plane wave. This has the form [2]

$$\tilde{\mathbf{E}}(t) = \tilde{\mathbf{E}}_0 e^{-i\omega t} + c.c., \quad (1)$$

where  $\tilde{\mathbf{E}}_0 = \mathbf{E}_0 e^{i(\mathbf{k}\cdot\mathbf{r}+\delta)}$  is the complex wave amplitude,  $\delta$  is the phase shift, and  $\mathbf{E}_0$  is the actual electric field amplitude, usually given in units of  $\frac{N}{C}$  or  $\frac{V}{m}$ . Because waves obey the principle of superposition,

two incident beams of different frequencies would combine to give [2]

$$\tilde{\mathbf{E}}_{\text{net}} = \tilde{\mathbf{E}}_1 e^{-i\omega_1 t} + \tilde{\mathbf{E}}_2 e^{-i\omega_2 t} + c.c., \quad (2)$$

where  $\tilde{\mathbf{E}}_1 = \mathbf{E}_1 e^{i(\mathbf{k}_1 \cdot \mathbf{r} + \delta_1)}$  and  $\tilde{\mathbf{E}}_2 = \mathbf{E}_2 e^{i(\mathbf{k}_2 \cdot \mathbf{r} + \delta_2)}$ . These equations describe fields of just the incident light. For electric fields traveling through a medium, it is necessary to introduce the polarization of the medium, which to the first order is given by the relationship [2]

$$\tilde{\mathbf{P}}(t) = \chi^{(1)} \tilde{\mathbf{E}}(t), \quad (3)$$

where  $\chi^{(1)}$  is known as the linear susceptibility. More generally, the polarization is actually a nonlinear process described by a power series expansion of the field strength. This is written mathematically as [2]

$$\tilde{\mathbf{P}}(t) = \chi^{(1)} \tilde{\mathbf{E}}(t) + \chi^{(2)} \tilde{\mathbf{E}}^2(t) + \chi^{(3)} \tilde{\mathbf{E}}^3(t) + \dots \quad (4)$$

$$\equiv \tilde{\mathbf{P}}^{(1)}(t) + \tilde{\mathbf{P}}^{(2)}(t) + \tilde{\mathbf{P}}^{(3)}(t) + \dots \quad (5)$$

For the case where there are two frequencies incident on a medium characterized by a second-order nonlinear susceptibility, the electric field is given by Eq. 2, only the second-order polarization is relevant, and there are actually five components of  $\tilde{\mathbf{P}}^{(2)}$ . This is due to the second-order non-linear polarization which is dependent upon the square of  $\tilde{\mathbf{E}}_{\text{net}}$ . Each component of  $\tilde{\mathbf{P}}^{(2)}$  refers to a different frequency which can be created in the medium. These components and their acronyms are given by [2]

$$P(2\omega_1) = \chi^{(2)} E_1^2 \quad (\text{SHG}) \quad (6)$$

$$P(2\omega_2) = \chi^{(2)} E_2^2 \quad (\text{SHG}) \quad (7)$$

$$P(\omega_1 + \omega_2) = 2\chi^{(2)} E_1 E_2 \quad (\text{SFG}) \quad (8)$$

$$P(\omega_1 - \omega_2) = 2\chi^{(2)} E_1 E_2^* \quad (\text{DFG}) \quad (9)$$

$$P(0) = 2\chi^{(2)} (E_1 E_1^* + E_2 E_2^*) \quad (\text{OR}) \quad (10)$$

where  $E^*$  is the complex conjugate of  $E$ . Equations 6 and 7 say that it is possible to create an electromagnetic wave with twice the frequency of waves one and two respectively. This process is known as second harmonic generation, or SHG. Similarly, Eq. 8 says that it is possible to create an electromagnetic wave with a frequency equal to the sum of the input frequencies and Eq. 9 says that it is possible to create

an electromagnetic wave with a frequency equal to the difference in input frequencies. These processes are known as sum frequency generation, SFG, and difference frequency generation, DFG, respectively. Finally, Eq. 10 says that it is possible to create a static polarization in the material with zero frequency. This is known as optical rectification, or OR. The total polarization is given by the sum of each of the components above.

## 2.0.2 Non-Linear Optics and SPDC

More relevant to this experiment, the process of spontaneous parametric down-conversion, SPDC, is similar to the process of DFG, but in reverse. This is shown schematically in Figure 1. One beam with frequency  $\omega_1$  is incident on the crystal, and two beams with  $\omega_2 = \omega_3 = \frac{\omega_1}{2}$  are emitted. The photons obey both

$$\omega_1 = \omega_2 + \omega_3 \quad \& \quad \mathbf{k}_1 = \mathbf{k}_2 + \mathbf{k}_3; \quad (11)$$

these are simply statements of conservation of energy and momentum respectively, as  $E_{\text{photon}} = \hbar\omega$  and  $\mathbf{p}_{\text{photon}} = \hbar\mathbf{k}$ .

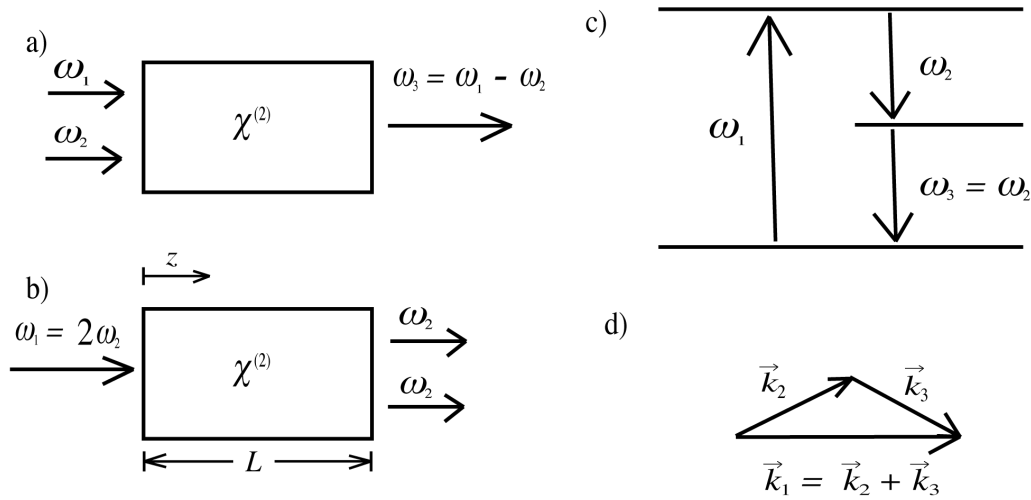


Figure 1: a) General DFG, b) SPDC with crystal geometry, c) Energy level diagram for SPDC, d) Momentum conservation for SPDC



See Boyd's Nonlinear Optics text, [2], for a complete derivation of the following discussion. Assuming a lossless medium, the net electric field inside the crystal for two electromagnetic waves is given by

$$\tilde{\mathbf{E}}_{net} = E_1 e^{-i\omega_1 t} + E_2 e^{-i\omega_2 t} + c.c., \quad (12)$$

where  $E_j = A_j(z) e^{ik_j z}$  and  $A_j$  is a slowly varying electric field amplitude. The wavenumber and refractive index for each frequency are given respectively by

$$k_j = \frac{n_j \omega_j}{c} \quad \& \quad n_j = \left[ \epsilon^{(1)}(\omega_j) \right]^{\frac{1}{2}}, \quad (13)$$

where  $\epsilon^{(1)}(\omega_j)$  is the dielectric permittivity tensor. The total intensity of the two beams is  $I = I_1 + I_2$ , where

$$I_j = \frac{P_j}{\pi w_0^2} = \frac{n_j c}{2\pi} A_j^2. \quad (14)$$

$P_j$  is the power due to each beam, and  $w_0$  is the focal spot size. To simplify the math, Boyd introduces new normalized field amplitudes  $u_1$  and  $u_2$  such that

$$u_1^2(\xi) + u_2^2(\xi) = 1, \quad (15)$$

where

$$\xi = \frac{z}{l} \quad \text{and} \quad l = \left( \frac{n_1^2 n_2 c^3}{2\pi I} \right)^{\frac{1}{2}} \frac{1}{8\pi \omega_1 d_{\text{eff}}}. \quad (16)$$

$\xi$  is called the normalized distance parameter,  $l$  is the characteristic distance over which the fields exchange energy, and  $d_{\text{eff}} = \frac{\chi^{(2)}}{2}$ . Using the driven non-linear wave equation, it can be shown with some lengthy algebra that the normalized field amplitudes are given by

$$u_1(\xi) = \text{sech} \xi \quad (17)$$

$$u_2(\xi) = \tanh \xi. \quad (18)$$

When the beam is at optimal focusing, the normalized distance parameter is

$$\xi = \left( \frac{1024\pi^5 d_{\text{eff}}^2 LP}{n_1 n_2 c \lambda_1^3} \right)^{\frac{1}{2}}, \quad (19)$$

and the conversion efficiency for this process is given by

$$\eta = \frac{u_2^2\left(\frac{L}{l}\right)}{u_1^2(0)} = \tanh^2\left(\frac{L}{l}\right). \quad (20)$$

For typical values, this efficiency turns out to be around 2%.

### 2.0.3 Phase Matching

Not only is the efficiency of this process somewhat low, but it requires a very precise matching of the wavevectors for the input and output beams. For SPDC, the wavevector mismatch is defined as

$$\Delta k \equiv k_1 - 2k_2, \quad (21)$$

where  $k_1$  is the the wavevector of the input beam and  $k_2$  is the wavevector of the output beam. The intensity of the output beam depends on  $\Delta k$  as

$$I_2 = I_2(\max) \frac{\sin^2\left(\frac{\Delta k L}{2}\right)}{\left(\frac{\Delta k L}{2}\right)^2} = I_2(\max) \operatorname{sinc}^2\left(\frac{\Delta k L}{2}\right). \quad (22)$$

In order to maximize the intensity of the down-converted beam, it is necessary to minimize  $\Delta k$ . It is possible do to this a few different ways, but the simplest is called angle tuning. This method involves precise angular orientation of the crystal with respect to the propagation direction of the incident light. Reference [2] describes the case of a uniaxial crystal, which pertains to this experiment. Uniaxial crystals are described by a particular direction known as the optic axis (or  $c$  axis). Light polarized perpendicular to the plane containing the propagation vector  $\mathbf{k}$  and the optic axis is called the ordinary polarization. Such light experiences the ordinary refractive index  $n_o$ . Light polarized in the plane containing  $\mathbf{k}$  and the optic axis is called the extraordinary polarization and experiences a refractive index  $n_e(\theta)$  which depends on the angle  $\theta$  between the optic axis and  $\mathbf{k}$  according to the formula

$$\frac{1}{n_e(\theta)^2} = \frac{\sin^2\theta}{\bar{n}_e^2} + \frac{\cos^2\theta}{n_o^2}. \quad (23)$$

The parameter  $\bar{n}_e$  is the principle value of the extraordinary refractive index. Note that  $n_e = \bar{n}_e$  when  $\theta = 90^\circ$  and  $n_e = n_o$  when  $\theta = 0^\circ$ . The extraordinary refractive index can be tuned by changing  $\theta$  to ensure that  $\Delta k = 0$ . The angle  $\theta$  is depicted in Figure 2. Depending on the polarization of the output beams, there are two types of phase matching. Type I phase matching is the case in which the two lower-frequency beams (in this case  $\omega_2 = \omega_3$ ) have the same polarization, and type II is the case where the polarizations are orthogonal. Differences between the two types are shown in Table 2. In the quantum photon model, individual incident photons are being split into two photons within the crystal, each with half the energy and thus half the frequency. These photons experience quantum entanglement, meaning

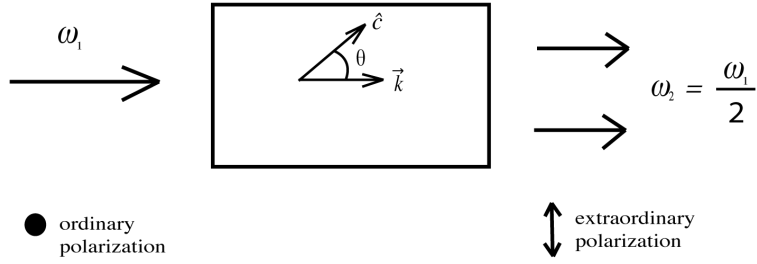


Figure 2: Phase matching angle  $\theta$  for SPDC where the ordinary polarization is normal to the page, and the extraordinary polarization is in the plane of the page as illustrated.

	Positive uniaxial ( $n_e > n_o$ )	Negative uniaxial ( $n_e < n_o$ )
Type I	$n_3^o \omega_3 = n_1^e \omega_1 + n_2^e \omega_2$	$n_3^e \omega_3 = n_1^o \omega_1 + n_2^o \omega_2$
Type II	$n_3^o \omega_3 = n_1^o \omega_1 + n_2^e \omega_2$	$n_3^e \omega_3 = n_1^e \omega_1 + n_2^o \omega_2$

Table 2: Type I vs Type II Phase Matching

the state of each photon is dependent of the other photon's state, and their intrinsic quantized spins are always opposite. For this experiment, type I phase matching occurs in a negative uniaxial crystal, so the phase matching condition is

$$n_e(2\omega, \theta) = n_o(\omega). \quad (24)$$

Using this condition, Eq. 23, and some trigonometry, the angle for ideal phase matching is found to be

$$\sin^2\theta = \frac{\frac{1}{n_o(\omega)^2} - \frac{1}{n_o(2\omega)^2}}{\frac{1}{n_e(2\omega)^2} - \frac{1}{n_o(2\omega)^2}}. \quad (25)$$

As the pairs of photons exit the crystal, they may do so with some relative angle between their paths. In general, this angle is given by the equation [1]

$$n_1 k_1 = 2n_2 k_2 \cos\theta_c. \quad (26)$$

Because  $k_2 = \frac{k_1}{2}$ , this simplifies to

$$\cos\theta_c = \frac{n_1}{n_2}, \quad (27)$$

which means that when perfect phase matching is achieved,  $n_1 = n_2$  and  $\theta_c = 0^\circ$ .

## 3 Experiment

### 3.1 List of Equipment

Item	Use
405 nm Diode Laser	Laser Source
Thorlabs Diode Laser Controller (LDC202)	Laser control
632 nm HeNe Laser	Alignment
Ortec Fast Coincidence Module (414A)	Detecting pairs of down-converted photons
Ortec Dual Counter/Timer (994)	Counting Coincident pairs
Ortec Single Channel Analyzer (406A) x 2	Analog to Digital signal conversion
Michelson Interferometer	Overlay an interference pattern on the output beam
Newport Universal Motion Controller (ESP300)	changing arm length in Michelson
Kikusui 20 MHz Storage Oscilloscope (COS5020-ST)	Signal Analysis
Perkin-Elmer Avalanche Photodiodes (SPCM-AQRH-13) x 2	Low-intensity photon detection

Table 3: Equipment

### 3.2 Experimental Setup

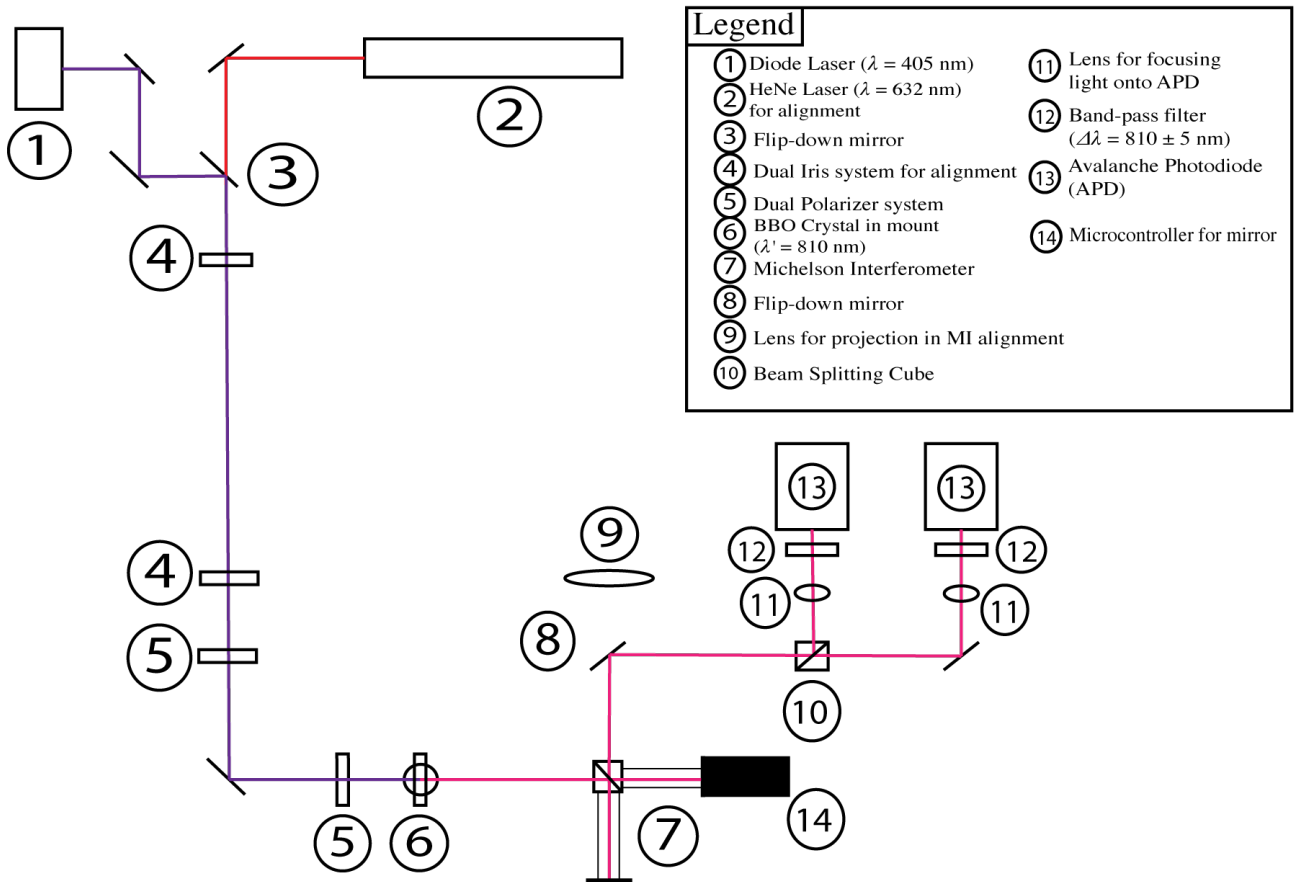


Figure 3: Optical Path Block Diagram

#### 3.2.1 Optics

The optical setup for this experiment begins with two lasers: a 632 nm HeNe laser for alignment and a 405 nm diode laser which acts as  $\omega_1$ . To ensure that the beams travel exactly the same path, a dual iris system is used. Each beam travels through the same two pinholes early on in the beam path, ensuring that

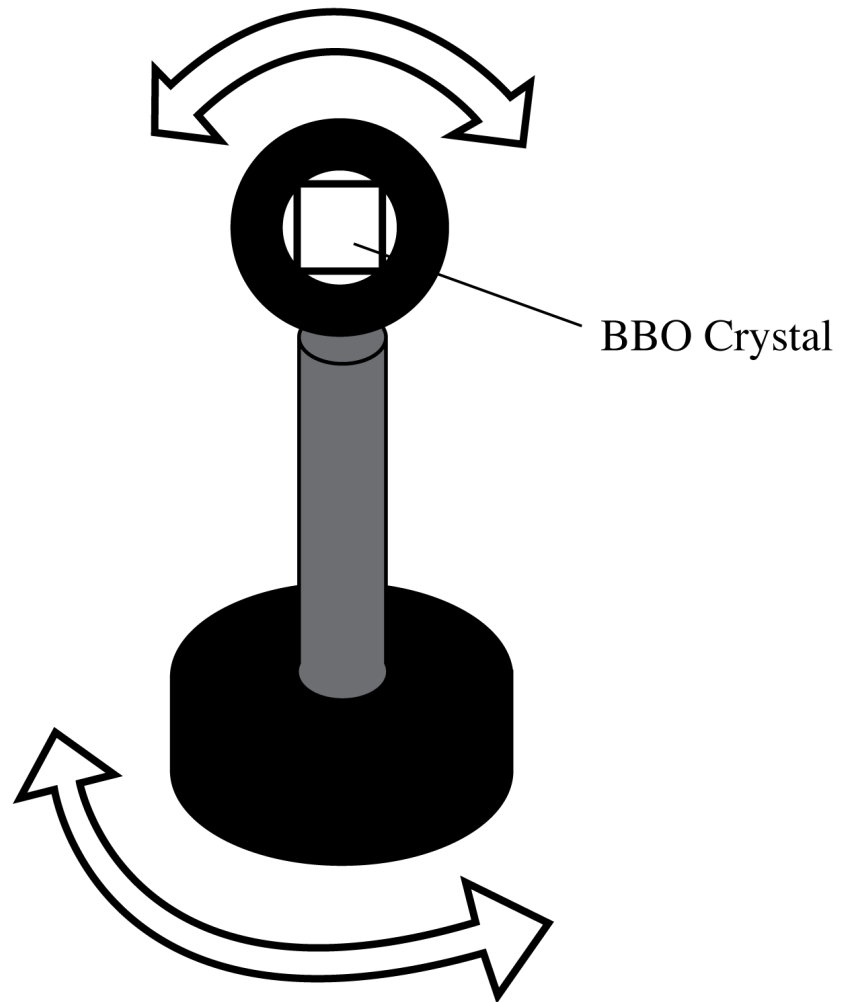
they are collinear. Thus the system can be aligned with the “easy-to-see” HeNe laser and still work for its less visible counterpart. The beam then goes through two polarizers to give the beam a known polarization and intensity control. After the polarizers, the beam is sent through the BBO crystal, which is in a mount with two rotational degrees of freedom. Section 3.2.2 describes the crystal and its mount. After the crystal, the relevant beam has a wavelength of 810 nm. For this reason, the mirrors after the BBO crystal have a dielectric coating for near infrared light, while the mirrors before the crystal are coated for light with a wavelength closer to the ultraviolet. The beam is then sent into a Michelson interferometer in order to create an arm-length dependent interference pattern in the output signal. The arm length in the interferometer is motion controlled, so very precise distance changes can be measured. The output is then sent through either a converging lens to expand the beam for alignment of the interferometer, or to a pair of Avalanche Photodiodes for detection. This is achieved through the use of a flip-down mirror. There is still a high intensity of 405 nm light in the beam path, so narrow bandpass filters are placed in front of the APD’s. These filters only let light with a wavelength of  $810 \pm 5$  nm pass through, and thus only the down-converted photons will be counted.

### 3.2.2 BBO Crystal

The BBO crystal is mounted such that the beam is at normal incidence, and the mount setup has two rotational degrees of freedom: the crystal can be rotated along the axis formed by the normal of the crystal face, as well as along the axis formed by the post supporting it. This is to match the polarization of the beam with the crystal axis and to make slight adjustments to the angle of incidence if necessary. The crystal is manufactured by PHOTOP, and consists of two BBO crystals that measure  $7 \times 7 \times 0.1$  mm, are cut at 29 degrees with respect to the optic axis of the crystal, P-coated for optimal transmission at 810 and 405 nm and mounted together with 90 degrees rotated between them. This allows for the beam to come in at normal incidence as mentioned before, which greatly simplifies the optical setup required. The down converted photons are thus collinear with the pump beam,  $\theta_c = 0^\circ$ . Finally, the crystal is a negative uniaxial crystal designed for Type I phase matching, which means that the ordinary and extraordinary indices of refraction and the various frequencies are related with  $n_e > n_o$  via

$$n_3^e \omega_3 = n_1^o \omega_1 + n_2^o \omega_2. \quad (28)$$

Adjustment of phase matching angle



Adjustment of incident angle

Figure 4: Mount for BBO crystal

### 3.2.3 Electronics

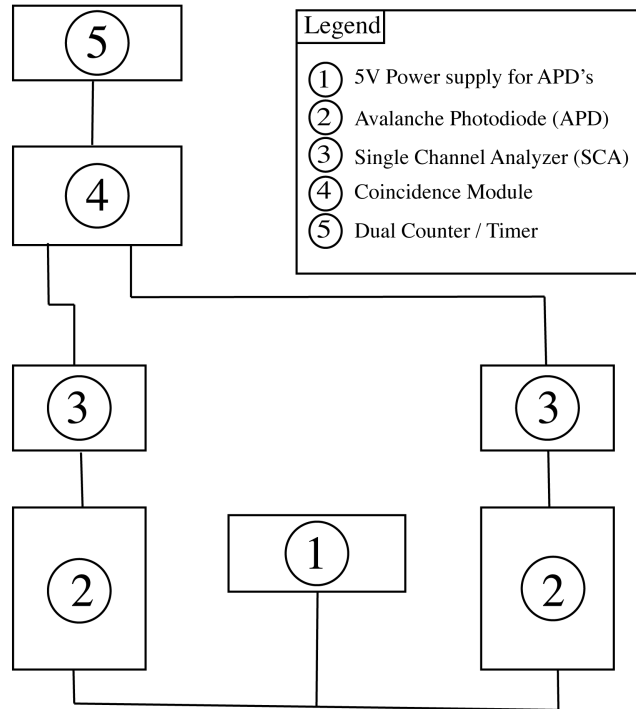


Figure 5: Block diagram of electronics showing the how coincidence counts are obtained from the APD's.

The first and most important components of the electronics for this experiment are the avalanche photodiodes. APD's are extremely sensitive light detectors, capable of detecting single photons. It is very important to keep light levels very low when the APD's are powered up with their detectors exposed, because too much light can render the APD broken and worthless. The APD's are thus always protected by a wooden box that is bolted to the table to cover them. An APD works by outputting an analog electrical pulse for every photon detected. The APD's used for this experiment output TTL pulses 35 ns wide that have a peak of at least 2.5-V in a 50- $\Omega$  load. There are 50 ns of dead time between pulses. The APD's require a 5-V supply with a current of around 0.5 A (1.9 A max). The pulses from the APD's are then sent into single channel analyzers to convert the pulses into a digital signal composed of step-functions. These cleaner signals are easier to count and are sent into a coincidence module to



register only coincident events. The output of the coincidence module is then sent to a counter to keep track of coincidence counts and count rates. If all goes right, the counter will show the number of pairs of down-converted photons. In addition to the previously mentioned electronics, an oscilloscope and function generator were used for testing, and a motion controller was used to change the arm length of the MI.

### **3.3 Procedures**

In order to take meaningful quantitative data, the optical system must be perfectly aligned for phase matching to occur. Once that happens, a number of different experiments can be performed with the down-converted photons. For an example, the arm-length of the Michelson Interferometer can be varied in order to create a pattern of constructive and destructive interference at the detector. This pattern can be seen by observing the number of coincidence counts at different arm lengths. See [1] for other possible experiments. Unfortunately there was not enough time to properly build, align, test, and get experimental data. A lot of time was spent designing and fabricating a box to fit in the tight space around the APD's, and the optical setup was so sensitive that it had to be re-aligned nearly every time it was used. Because of the shortage of time and difficulty in alignment, phase matching was never achieved and SPDC was never actually detected. Given more time however, phase matching could certainly be attained and down-converted photons could be detected by the APD's.

## **4 Conclusions**

In conclusion, the experiment was set up but not yet perfectly aligned. Once it is aligned and phase matching occurs, a number of experiments can be done with relative ease. Despite not finishing the project and getting any data, I have learned a lot about theoretical and experimental non-linear quantum optics, electronics, and signal processing. Additionally, this project has given me invaluable experience in the flow of and dedication required to do research in experimental physics. The process is filled with surprises, successes, and failures; a researcher never knows exactly what is going to happen next.

## **5 Future Work**

After I graduate, I hope to continue working on refining this project as a Masters student in Electrical Engineering. There are a number of additional experiments that can be done with the entangled photons exiting the crystal, and for this reason we are working to make this experiment a part of the advanced Quantum Laboratory curriculum. This would be done by automating the data collection process using Labview, in order to more easily take data and make this an approachable experiment for most undergraduate physics majors.

## References

- [1] E. J. Galvez et al, Am. J. Phys **73**, Feb (2004).
- [2] R. W. Boyd, *Nonlinear Optics*, Second Edition, (Academic Press, San Diego, CA, 2003.)
- [3] F. L. Pedrotti, L. S. Pedrotti, and L. M. Pedrotti, *Introduction to Optics*, Third Edition, (Person Prentice Hall, Upper Saddler River, NJ, 2007.)